Atmos. Chem. Phys. Discuss., 15, 28453–28482, 2015
www.atmos-chem-phys-discuss.net/15/28453/2015/
doi:10.5194/acpd-15-28453-2015


Atmospheric Chemistry and Physics Discussions



# Light absorption of brown carbon aerosol in the PRD region of China

**J.-F. Yuan, X.-F. Huang, L.-M. Cao, J. Cui, Q. Zhu, C.-N. Huang, Z.-J. Lan, and L.-Y. He**

Key Laboratory for Urban Habitat Environmental Science and Technology, School of Environment and Energy, Peking University Shenzhen Graduate School, Shenzhen 518055, China

Received: 2 September 2015 – Accepted: 14 October 2015 – Published: 21 October 2015

Correspondence to: X.-F. Huang (huangxf@pku.edu.cn)

Published by Copernicus Publications on behalf of the European Geosciences Union.







## Abstract

The strong spectral dependence of light absorption of brown carbon (BrC) aerosol is regarded to influence aerosol's radiative forcing significantly. The Absorption Angstrom Exponent (AAE) method was widely used in previous studies to attribute light absorption of BrC at shorter wavelengths for ambient aerosol, with a theoretical assumption that the AAE of "pure" black carbon (BC) aerosol equals to 1.0. In this study, the previous AAE method was improved by statistical analysis and applied in both urban and rural environments in the Pearl River Delta (PRD) region of China. A three-wavelength photo-acoustic soot spectrometer (PASS-3) and aerosol mass spectrometers (AMS) were used to explore the relationship between the measured AAE and the relative abundance of organic aerosol to BC. The regression and extrapolation analysis revealed that the more realistic AAE values for "pure" BC aerosol were 0.86, 0.82, and 1.02 at 405 nm, and 0.70, 0.71, and 0.86 at 532 nm, in the campaigns of $urban_{\_winter}$, $urban_{\_fall}$, and $rural_{\_fall}$, respectively. Roadway tunnel experiments were also conducted, and the results further supported the representativeness of the obtained AAE values for "pure" BC aerosol in the urban environments. Finally, the average aerosol light absorption contribution of BrC was quantified to be 11.7, 6.3, and 12.1 % (with relative uncertainties of 4, 4, and 7 %) at 405 nm, and 10.0, 4.1, and 5.5 % (with relative uncertainties of 2, 2, and 5 %) at 532 nm, in the campaigns of $urban_{\_winter}$, $urban_{\_fall}$, and $rural_{\_fall}$, respectively. The relatively higher BrC absorption contribution at 405 nm in the $rural_{\_fall}$ campaign was likely a result of the biomass burning events nearby, which was supported by the biomass burning simulation experiments performed in this study. The results of this paper indicate that the brown carbon contribution to aerosol light absorption at shorter wavelengths is not negligible in the highly urbanized and industrialized PRD region.





ACPD
15, 28453–28482, 2015



## 1 Introduction

Light absorbing carbonaceous aerosols including black carbon (BC) and brown carbon (BrC) are the primary matters absorbing light in the atmosphere. The importance of BC has been widely recognized in recent decades due to its effects of radiative forcing on climate change while that of BrC is far from being well known comparatively. (Jacobson, 2001; Hansen et al., 1997; Haywood et al., 1997; Ramanathan and Carmichael, 2008; Gadhavi and Jayaraman, 2010; Wang et al., 2014). Brown carbon is the organic carbon which can absorb light based on a variety of chemical structures like nitrated/polycyclic aromatics, phenols, humic-like substances and biopolymers, etc. (Jacobson, 1999; Sun et al., 2011; Poschl, 2005). It mainly absorbs light at UV and short-visible wavelengths (Chen and Bond, 2010; Kirchstetter et al., 2004; Lewis et al., 2008; Sandradewi et al., 2008c; Schmid et al., 2006) and this strong spectral dependence has aroused more and more interest recently (Feng et al., 2013; Bahaduret al., 2012; Chung et al., 2012b; Wang et al., 2014; Jethva et al., 2011). BrC aerosol was estimated to contribute about 10–30 % of total absorption of fine particles at shorter wavelengths, e.g., at 365, 404, or 405 nm, and around 10 % at mid-visible wavelengths, e.g., at 532 nm (Bahadur et al., 2012; Lack et al., 2012b; Washenfelder et al., 2015; Nakayama et al., 2014). During an agricultural waste burning event, BrC aerosol could contribute more than 65 and 15 % light absorption at 370 nm and mid-visible wavelengths, respectively (Favez et al., 2009). However, the complexity and variety of molecular composition of BrC and the mixing state with other substances make it very challenging to study its optical properties (Alexander et al., 2015). Main sources for BrC include biomass and biofuel burning, atmospheric humic-like substances (HULIS) from multiple phase actions and photochemical oxidation of volatile organic compounds (VOCs; Bond, 2001; Bergstrom et al., 2007; Alexander et al., 2015). In East Asia, one of the five regions of atmospheric brown clouds (ABC), biomass burning was found not to be the only source of BrC (Miyazaki et al., 2007; Kirillova et al., 2014; Du et al., 2014a, b; Cheng et al., 2011, 2012, 2013). Extensive experimental data from field studies are essential to





ACPD
15, 28453–28482, 2015



evaluate light absorption by brown carbon as well as constraining and validating future atmospheric and climate models.

There were two main methods to identify the absorption of BrC in total absorption at shorter wavelengths in previous studies: one used theoretical Mie models to calculate the light absorption of BrC aerosol with the input of ambient chemical, physical, and optical measurements of the bulk aerosol (Lack et al., 2012b). The other method was based on the optical measurements followed by Absorption Angstrom Exponent (AAE) calculation, which seemed more simple and universal by using a criterion AAE for "pure" BC aerosol ($AAE_{BC}$; Fialho et al., 2005; Clarke et al., 2007; Sandradewi et al., 2008a, b; Favez et al., 2009; Yang et al., 2009; Jayaraman., 2010; Herich et al., 2011; McNaughton et al., 2011; Bahadur et al., 2012; Chung et al., 2012a; Esposito et al., 2012; Gadhavi and Wang et al., 2013; Cazorla et al., 2013). The $AAE_{BC}$ has been commonly assumed to be 1.0 theoretically in different places and periods, but this simple assumption may not be reliable and could cause possible bias of the attributed absorption of BC from −22 to +7 %, which causes further uncertainties in the attributed absorption of BrC then (Lack and Langridge, 2013).

In this study, we tried to improve the AAE method through statistical analysis based on on-line determining the $AAE_{BC}$ in real ambient measurement campaigns. The improved AAE method was applied in both urban and rural areas in the Pearl River Delta (PRD) region of China, in order to attribute the light absorption of BrC there. The PRD region is one of the three economically-developed regions of China and has been considered as one of the world's largest sources of anthropogenic soot emissions (Streets et al., 2001; Bond et al., 2004; Koch and Hasen, 2005). Despite of the strong emissions of BC aerosol in the highly urbanized and industrialized PRD region, the light absorption contribution of BrC aerosol should not be neglected without effective evaluation. Therefore, the focus of this paper is to reasonably quantify the light absorption by BrC aerosol in PRD with uncertainty evaluation using an improved AAE method.





ACPD
15, 28453–28482, 2015



## 2 Experimental and data analysis methods

### 2.1 Sampling sites and periods

Our observations contain three field campaigns conducted in Shenzhen and Heshan in PRD, during the fall and winter seasons of 2014, which are usually the polluted dry seasons of PRD with high frequency of haze episodes. The Shenzhen site (SZ) is an urban site in the southeast of PRD region. It is on the campus of Peking University Shenzhen Graduate School (22.60° N, 113.97° E) located in the west of Shenzhen and the sampling periods were from 15 January to 19 February in the winter (urban$_{_winter}$) and from 12 September to 9 October in the fall (urban$_{_fall}$). The Heshan site (HS) is a rural site (22.71° N, 112.93° E) 40–50 km southwest of Guangzhou megacity in the central PRD. It is located on the top of a small hill with little local emission except biomass burning. The HS sampling period was from 1 November to 22 November in the fall (rural$_{_fall}$) and biomass burning events were observed occasionally as an obvious anthropogenic source in the nearby farmland.

In addition, tunnel experiments were also performed in Shenzhen during 2014 to explore the AAE values in a more BC-polluted environment. The tunnel experiments were performed three times inside two roadway tunnels in Shenzhen urban areas. One of the tunnels is the Tanglangshan tunnel (TL), and the sampling periods were from 0:00 to 5:30 am on 16 and 18 October (TL-1 and TL-2). The TL tunnel is 1.71 km in length, with two channels that has three lanes in one direction for traffic, and the driving speeds in the tunnel are usually between 50–60 km/h. The monitoring car was located 400 m in depth from the entrance. The other tunnel is the Jiuweiling tunnel (JW), and the sampling period was from 3:30 to 24:00 pm on 10 December. The JW tunnel is 1.45 km in length, with two channels that has two lanes in one direction for traffic, and the driving speeds in the tunnel are usually about 60 km/h. The monitoring car was located 800 m in depth from the entrance.

Moreover, biomass burning simulation experiments were previously performed in a combustion laboratory to study the spectral dependence in biomass burning smoke.





ACPD
15, 28453–28482, 2015



Different types of biomass materials including straw, deciduous leaf, and firewood were burned in two different combustion modes, i.e., stove burning and open burning, to simulate the traditional residential and field biomass burning in rural areas in the PRD region. The combustion system in the laboratory includes four parts: combustion simulation, dilution, tube sampling, and instrumental analyzing. The stove was built with bricks and mortar according to the local traditional structure. More detailed information of the combustion system was described in our previous paper (He et al., 2010). Different biomass materials were burned inside the stove to simulate a complete water heating process referring to the water boiling test protocol by the University of California (http://www.aprovecho.org/lab/pubs/testing). Besides, certain amount of straw was piled up and burned on a pallet made of iron wire to simulate the open burning of crop residue in the field.

## 2.2 Instrumentation

For all the sampling in this study, the instruments were placed in a temperature controlled room (or a monitoring car for the tunnel experiments), and the outdoor air was induced through a $PM_{2.5}$ cyclone inlet placed above the rooftop and then dried before it entered the inlets of the instruments. A three-wavelength Photo-acoustic Soot Spectrometer (PASS-3; Droplet Measurement Technologies, CO, USA) was used to measure light absorption at 405, 532, and 781 nm with a data time resolution of 2 min. The principles and technical details of PASS have been described previously in Arnott et al. (1999). Then, we processed the 2 min data for half hour averages in the later data analysis and discussion.

A high-resolution time-of-flight aerosol mass spectrometer (HR-ToF-AMS; Aerodyne Research, MA, US) was used to measure non-refractory species of $PM_1$ including organic aerosol with a time resolution of 10 min at the SZ site. The detailed description and general data processing are given in DeCarlo et al. (2006) and the calibration followed the standard protocols (Jayne et al., 2000; Jimenez et al., 2003; Drewnick et al., 2005). More details about the HR-ToF-AMS operation have been described in





ACPD
15, 28453–28482, 2015



our previous publications (He et al., 2011; Huang et al., 2011). An aerosol chemical speciation monitor (ACSM; Aerodyne Research, MA, US) which is a convenient version of HR-ToF-AMS, was used at the HS site and in the tunnel experiments to measure $PM_1$ with a time resolution of 10 min. The detailed description of ACSM was given in Ng et al. (2011).

### 2.3 Calibration of PASS-3

The calibrations of PASS-3, including those of flow rate, laser power, and absorption, were conducted following the standard procedures provided by the operational manual and satisfied results were obtained and summarized in Table 1. The absorption calibration showed good linear regression coefficients ($R^2 > 0.99$) and the calibration curve slopes were quite close to the theoretical value of 1 which proved that the instrument was stable enough and performed well in the campaigns. The detection limits of aerosol light absorption were 10, 10, and 3 $Mm^{-1}$ at 405, 532, and 781 nm, respectively.

### 2.4 Calculation of AAE and light absorption of brown carbon

The Absorption Angstrom Exponent (AAE) is an application of Angstrom exponent (Angstrom, 1929) to describe the wavelength dependence of visible light absorption by aerosol, as expressed in Eq. (1):

$$AAE = -\ln(Abs_{\lambda 1}/Abs_{\lambda 2})/\ln(\lambda 1/\lambda 2) \quad (1)$$

where Abs can be obtained by the absorption measurement, and $\lambda$ represents different wavelengths. The traditional AAE method for estimating BrC light absorption has been described previously by Lack and Langridge (2013), and it can be expressed in Eqs. (2) and (3):

$$BC_{Abs_{\lambda 1}} = Abs_{\lambda 2} \cdot (\lambda 2/\lambda 1)^{AAE_{BC}} \quad (2)$$

$$BrC_{Abs_{\lambda 1}} = Abs_{\lambda 1} - BC_{Abs_{\lambda 1}} \quad (3)$$





ACPD
15, 28453–28482, 2015



where $Abs_{\lambda 2}$ is the measured absorption at a longer wavelength ($\lambda 2$) at which BrC has negligible or no absorption. $BC_{Abs_{\lambda 1}}$ is the attributed absorption of BC at a shorter wavelength. $BrC\_Abs_{\lambda 1}$ is then the attributed absorption of BrC at the shorter wavelength. The $AAE_{BC}$ is referred as the AAE caused solely by "pure" BC aerosol, which was usually assumed to be 1.0 theoretically. The total uncertainty of $BrC_{Abs_{\lambda 1}}$ calculated ($U_t$) thus arises from both the AAE attribution method and the measurements, and can be estimated by Eq. (4):

$$U_t = \sqrt{(U_{Abs_{\lambda 1}})^2 + (U_{Abs_{\lambda 2}})^2 + (U_{AAE_{BC}} \cdot \ln(\lambda 2/\lambda 1))^2} \quad (4)$$

where $U_{AAE\_BC}$ is the absolute uncertainty of the $AAE_{BC}$ used, and $U_{Abs_{\lambda 1}}$ and $U_{Abs_{\lambda 2}}$ are the relative uncertainties of the absorption measured at $\lambda 1$ and $\lambda 2$, respectively. The $U_{Abs_{\lambda(1 \text{ or } 2)}}$ can be calculated following Eqs. (5) and (6):

$$\Delta X_{t_{min}} = \frac{1}{t/2} \cdot \sqrt[2]{\sum_0^t (\text{NoiseEqBabs}_{2min})^2} \quad (5)$$

$$U_{Abs_\lambda} = \Delta X_{t_{min}} / Abs_\lambda \quad (6)$$

where $NoiseEqBabs_{2min}$ is the noise equivalent absorption at a wavelength output by PASS-3 every 2 min, representing the absolute uncertainty for the corresponding aerosol absorption measured. For the average absorption of a longer period ($Abs_\lambda$), the absolute uncertainty ($\Delta X_{t_{min}}$) can be calculated through uncertainty propagation following Eq. (5). Then, the $\Delta X_{t_{min}}$ is divided by $Abs_\lambda$ to get the corresponding relative uncertainty ($U_{Abs_\lambda}$) as in Eq. (6).





ACPD
15, 28453–28482, 2015



## 3 Results and discussion

### 3.1 Aerosol light absorption

The time series of $PM_{2.5}$ light absorption at three wavelengths in the different campaigns are shown in Fig. 1. In the urban$_{_winter}$ campaign, the average absorption was $25.6 \pm 22.3$, $18.7 \pm 16.3$, and $12.9 \pm 11.4\,Mm^{-1}$ at 405, 532, and 781 nm, respectively. In the urban$_{_fall}$ campaign, the average absorption was $21.6 \pm 13.2$, $16.2 \pm 10.3$, and $11.8 \pm 7.6\,Mm^{-1}$ at 405, 532, and 781 nm, respectively. It is seen that the aerosol absorbed more light in the winter, and its maximum absorptions were 162, 122, and $86.6\,Mm^{-1}$ at 405, 532, and 781 nm, respectively, more than two times of the maximum values in the fall. The higher aerosol pollution level observed in the winter can be attributed to the unfavorable meteorological conditions in PRD in winter. The aerosol light absorption levels observed in urban SZ were much higher than those observed in urban Denver, Colorado, where the maximum values of absorption were less than $20\,Mm^{-1}$ at 532 and 685 nm (Moosmuller et al., 1998). In the rural$_{_fall}$ campaign, the average absorption was $32.5 \pm 18.3$, $21.5 \pm 12.0$, and $14.6 \pm 8.1\,Mm^{-1}$ at 405, 532, and 781 nm, respectively. These aerosol absorption levels were even higher than those of urban$_{_winter}$ and urban$_{_fall}$ campaigns, but this is not strange since HS is a receptor site, suffering from the severe polluted outflow air from its northeastern the Guangzhou megacity during the fall and winter seasons (Gong et al., 2012). The average ambient $AAE_{405\_781}$ values were calculated to be 1.05, 0.92, and 1.22, respectively for the urban$_{_winter}$, urban$_{_fall}$, and rural$_{_fall}$ campaigns, while those of $AAE_{532\_781}$ were 0.98, 0.82, and 1.00, respectively. The observed AAE values of less than 1.0 implies that the theoretical default AAE value of 1.0 for "pure" BC absorption is not realistic in PRD. On the other hand, the relatively higher value of $AAE_{405\_781}$ in the rural$_{_fall}$ campaign might be related to the biomass burning in the farmland nearby, which will be analyzed in Sect. 3.4.





ACPD
15, 28453–28482, 2015



It should be noted here that the contribution of dust particles to the aerosol light absorption is considered to be negligible in this study. Firstly, there were no dust events during the three campaigns, which actually scarcely happened in the PRD region of South China. Secondly, organic aerosol typically contributes > 30 % of $PM_{2.5}$ mass in Shenzhen, far higher than that of the dust (< 5 %; Huang et al., 2014). Considering that the mass absorption efficiency (MAE) values of dust at shorter and mid-visible wavelengths are lower than those of organic aerosol by a magnitude of one or two (Favez et al., 2009; Yang et al., 2009), the light absorption contribution of dust can be negligible in comparison with that of organic aerosol in urban$_{_winter}$ and urban$_{_fall}$ campaigns. It should be also the case in the rural$_{_fall}$ campaign since dust also contributes a small mass fraction (< 5 %) in the rural atmosphere in the PRD region (Huang et al., 2014). Therefore, the light absorption of dust is not taken into account in the following discussion.

### 3.2 Determination of the AAE for "pure" BC aerosol

Theoretically, the AAE for "pure" BC aerosol ($AAE_{BC}$) is assumed to be 1.0 (Lack and Langridge, 2013), and BrC absorption at shorter wavelengths can raise this value in ambient atmosphere. In this study, we explore the more realistic $AAE_{BC}$ in PRD by establishing a univariate regression relationship for each campaign, as shown in Fig. 2. In each campaign, the organic aerosol mass concentration was measured by AMS or ACSM, as shown in Fig. 1, and the absorption at 781 nm ($Abs_{781\,nm}$) could be used to represent the BC amount since brown carbon has negligible absorption at longer wavelengths (Kirchstetter et al., 2004; Lack and Langridge, 2013; Lack et al., 2012b). Then, $r_{org/bc}$ (representing the ratio of organic aerosol mass concentration to $Abs_{781\,nm}$) was used as an index of the relative abundance of organic aerosol to BC. Finally, the $AAE_{405\_781}$ and $AAE_{532\_781}$ were plotted versus the $r_{org/bc}$ averaged within equal intervals for each campaign in Fig. 2, with the corresponding linear fitting curves.

For all the campaigns, the linear relationships between $AAE_{405\_781}$ ($AAE_{532\_781}$) and $r_{org/bc}$ were significant enough with the correlation coefficients ($R^2$) of 0.59–0.98, in-





ACPD
15, 28453–28482, 2015



dicating AAE was positively related with the relative amount of organic matter, which certainly includes brown carbon. In addition, previous studies also showed that the AAE of aerosol in ambient air can be affected by a couple of other factors other than BrC, such as size distribution, mixing state, and fractal dimension of BC particles (Levin et al., 2010; Gyawali et al., 2009; Scarnatol et al., 2013; Bond et al., 2006), which can be partly reflected by the standard deviations of the data points in Fig. 2. The intercepts of the fitting curves in Fig.2, where $r_{org/bc} = 0$, can be regarded as the absorption of "pure" BC without any organic matter or brown carbon, and thus are suitable proxies of the $AAE_{BC}$ values for the different campaigns. The uncertainties of the regression intercepts represent the absolute uncertainties of the $AAE_{BC}$ ($U_{AAE\_BC}$), and can be calculated following Eq. (7):

$$U_{AAE_{BC}} = t_p \cdot S(a) \tag{7}$$

where $S(a)$ represents the standard deviation of the regression intercept ($a$) calculated by the SPSS software, and $t_p$ was determined by the $t$-distribution list according to the selected confidence level ($p$), which was set to be 95 % in this study.

The calculated $AAE_{BC}$ values and corresponding uncertainties at 405 and 532 nm are summarized in Table 2, and they are found similar in the $urban_{\_winter}$ ($0.86 \pm 0.06$ and $0.70 \pm 0.05$) and $urban_{\_fall}$ ($0.82 \pm 0.06$ and $0.71 \pm 0.06$) campaigns, but much higher in the $rural_{\_fall}$ campaign ($1.02 \pm 0.10$ and $0.86 \pm 0.13$). The difference of the $AAE_{BC}$ between the urban site and the rural site suggests different source structures of BC aerosol at the two sites. Fossil fuel combustion, e.g., vehicle emissions, was indicated to be the dominant source of BC aerosol in urban Shenzhen (Lan et al., 2011), while biomass burning emission played an important role in fall at the rural HS site (Gong et al., 2012). These results suggest that $AAE_{BC}$ can vary spatially, and the simple assumption of 1.0 for it is not reasonable enough.





ACPD
15, 28453–28482, 2015



### 3.3 AAE measurements for primary emission sources

#### 3.3.1 Roadway tunnel experiments

Since the primary source of BC in urban environment in PRD was proved to be vehicular exhaust (Yuan et al., 2006; Huang et al., 2006; Lan et al., 2013), we performed three roadway tunnel experiments in urban Shenzhen as described in Sect. 2.1, in order to verify the representativeness of the $AAE_{BC}$ derived for the urban SZ atmosphere. The tunnel air measurement results were similarly presented in Fig. 3. Since the tunnel air was expected to be largely dominated by fresh BC particles, the observed $r_{org/bc}$ is found to be in a lower range (about 0.2–0.8) in comparison with in the urban SZ atmosphere, and thus the extrapolation of the linear regression line in Fig. 3 can get a more reliable intercept, i.e., $AAE_{BC}$. As summarized in Table 3, the $AAE_{BC}$ values obtained at 405 and 532 nm (0.80–0.89 and 0.63–0.72, respectively) in the tunnel experiments well confirmed the $AAE_{BC}$ values derived from the ambient measurements at the urban SZ site.

#### 3.3.2 Biomass burning simulation experiments

Since the rural_fall campaign was observed to be influenced by biomass burning events, which are actually frequent in rural areas in PRD, especially in fall, we performed biomass burning simulation experiments, as described in Sect. 2.1, in order to explore the light absorption spectral dependence of biomass burning particles. The AAE values with standard deviation of different types of biomass burning were presented in Table 4. It was found that the absorption generally showed large spectral dependence, with $AAE_{405-781}$ ranging from 1.7–6.2 and $AAE_{532-781}$ ranging from 1.3–5.0, significantly higher than those observed in the ambient air and tunnel air. For the combustion type of stove burning, the leaves tended to emit more brown carbon than that of wood, stalk, and straw, which should be a result of their different biomass chemical nature. Besides, the AAE values of short straw were a few times higher in open burning than





ACPD
15, 28453–28482, 2015



in stove burning, which can be explained by that it is easier to cause a hypoxic environment in smoldering, and a large amount of yellow fume containing brown carbon can thus be produced (Einfeld et al., 1991; Patterson and McMahon, 1984; Kirchstetter et al., 2004; Chakrabarty et al., 2010). Therefore, the higher AAE values observed for biomass burning particles indicate that biomass burning should be an important source of BrC aerosol in PRD.

### 3.4 Quantification of light absorption of brown carbon

Based on the well determined $AAE_{BC}$ and $Abs_{781\,nm}$ in the three field campaigns, we can finally calculate the light absorption of "pure" BC and then BrC at 405 and 532 nm according to Equations 2 and 3. In result, the average light absorption of BrC were 3.0, 1.4, and 3.9 $Mm^{-1}$ at 405 nm and 1.9, 0.7, and 1.2 $Mm^{-1}$ at 532 nm in the $urban_{\_winter}$, $urban_{\_fall}$, and $rural_{\_fall}$ campaigns, respectively, corresponding to 11.7, 6.3, and 12.1 % at 405 nm and 10.0, 4.1, and 5.5 % at 532 nm of the total aerosol light absorption, respectively. The associated uncertainties were estimated following Equation 4, and small relative uncertainties of 4, 4, and 7 % at 405 nm and 2, 2, and 5 % at 532 nm were obtained for the $urban_{\_winter}$, $urban_{\_fall}$, and $rural_{\_fall}$ campaigns, respectively.

The results indicate that no matter at the urban site or rural site in PRD, BC still plays a dominant role in the total aerosol light absorption at 405 and 532 nm, but the contribution from BrC is not negligible, with a level of up to 12 %. The higher proportion of BrC contribution in the $urban_{\_winter}$ campaign than that in the $urban_{\_fall}$ campaign suggests that BrC could play a more important role under more polluted conditions. On the other hand, the higher BrC contribution at 405 nm in the $rural_{\_fall}$ campaign is very likely related to the influence of biomass burning in the farmland nearby, which is supported by its larger difference of BrC absorption between 405 and 532 nm. The $AAE_{405\_532}$ were calculated to be 1.05, 1.15, and 1.52 for the $urban_{\_winter}$, $urban_{\_fall}$, and $rural_{\_fall}$ campaigns, respectively, and the higher $AAE_{405\_532}$ in the $rural_{\_fall}$ campaign is consistent with the higher $AAE_{405\_532}$ obtained in the biomass burning simulation





ACPD
15, 28453–28482, 2015



experiments in Table 4. The especially strong absorption at 404 nm of biomass burning brown carbon was also found by Lack et al. (2012b).

Finally, it should be noted that it is unwise to calculate the light absorption contribution of BrC at a specific time during the field campaigns, since the $AAE_{BC}$ derived for the average case of a single campaign in section 3.2 could have large bias from the real $AAE_{BC}$ at that time, due to the variations of the influencing factors, e.g., size distribution, mixing state, and morphology of BC particles.

## 4 Conclusions

In this study, an improved AAE method was used to estimate the light absorption of brown carbon at an urban site and a rural site in PRD region of China in the polluted seasons during 2014, based on ambient on-line measurements using PASS-3, AMS (or ACSM). The measured $AAE_{405\_781}$ averages were 1.05, 0.92, and 1.22, and those of $AAE_{532\_781}$ were 0.98, 0.82, and 1.00 in the three campaigns of $urban_{\_winter}$, $urban_{\_fall}$, and $rural_{\_fall}$, respectively. The linear regression between $AAE_{405\_781}$ (and $AAE_{532\_781}$) and the ratio of organic aerosol to BC for each campaign resulted in reasonable intercepts, which were assumed to represent the absorption of "pure" BC at 405 and 532 nm. The obtained AAE values for "pure" BC ($AAE_{BC}$) were $0.86 \pm 0.06$, $0.82 \pm 0.06$, and $1.02 \pm 0.10$ at 405 nm, and $0.70 \pm 0.05$, $0.71 \pm 0.06$, and $0.86 \pm 0.13$ at 532 nm in the campaigns of $urban_{\_winter}$, $urban_{\_fall}$, and $rural_{\_fall}$, respectively. They are believed to be more realistic in PRD than the theoretical default value of 1.0. The results from the tunnel experiments further confirmed that the $AAE_{BC}$ values in the SZ urban atmosphere should be within the range of 0.8–0.9 and 0.6–0.7 at 405 and 532 nm, respectively. The calculated light absorption contributions of brown carbon were 11.7, 6.3, and 12.1 % at 405 nm, and 10.0, 4.1, and 5.5 % at 532 nm of the total aerosol absorption, in the campaigns of $urban_{\_winter}$, $urban_{\_fall}$, and $rural_{\_fall}$, respectively, with relative uncertainties of 4, 4, and 7 % at 405 nm, and 2, 2, and 5 % at 532 nm, respectively. It was found that BrC played a more important role in the more polluted season or in the rural





ACPD
15, 28453–28482, 2015



area significantly influenced by biomass burning in the PRD region. Although BC still played a dominant role in aerosol light absorption in PRD, the contribution of BrC at shorter wavelengths is not negligible, with a level of up to above 10 %.

*Acknowledgements.* This work was supported by the National Natural Science Foundation of China (21277003 & U1301234), the Ministry of Science and Technology of China (2013CB228503), and the Science and Technology Plan of Shenzhen Municipality.

## References

Alexander, L., Julia, L., and Serger, A. N.: Chemistry of Atmospheric Brown Carbon, Chem. Rev., 115, 4335–4376, 2015.

Ångström, A.: On the Atmospheric Transmission of Sun Radiation and on Dust in the Air, Geografika Ann., 11, 156–166, 1929.

Arnott, W. P., Moosmuller, H., Rogers, C. F., Jin, T. F., and Bruch, R.: Photoacoustic spectrometer for measuring light absorption by aerosol: instrument description, Atmos. Environ., 33, 2845–2852, 1999.

Arola, A., Schuster, G., Myhre, G., Kazadzis, S., Dey, S., and Tripathi, S. N.: Inferring absorbing organic carbon content from AERONET data, Atmos. Chem. Phys., 11, 215–225, doi:10.5194/acp-11-215-2011, 2011.

Bahadur, E., Praveen, P. S., Xu, Y., and Ramanathan, V.: Solar absorption by elemental and brown carbon determined from spectral observations, P. Natl. Acad. Sci. USA, 109, 17366–17371, 2012.

Bergstrom, R. W., Pilewskie, P., Russell, P. B., Redemann, J., Bond, T. C., Quinn, P. K., and Sierau, B.: Spectral absorption properties of atmospheric aerosols, Atmos. Chem. Phys., 7, 5937–5943, doi:10.5194/acp-7-5937-2007, 2007.

Bond, T. C.: Spectral dependence of visible light absorption by carbonaceous particles emitted from coal combustion, Geophys. Res. Lett., 28, 4075–4078, 2001.

Bond, T. C. and Bergstrom, R. W.: Light Absorption by Carbonaceous Particles: An Investigative Review, Aerosol Sci. Technol., 40, 27–67, doi:10.1080/02786820500421521, 2006.

Bond, T. C., Streets, D. G., Yarber, K. F., Nelson, S. M., Woo, J. H., and Klimont, Z.: A technology-based global inventory of black and organic carbon emissions from combustion, J. Geophys. Res., 109, D14203, doi:10.1029/2003jd003697, 2004.





ACPD
15, 28453–28482, 2015



Cazorla, A., Bahadur, R., Suski, K. J., Cahill, J. F., Chand, D., Schmid, B., Ramanathan, V., and Prather, K. A.: Relating aerosol absorption due to soot, organic carbon, and dust to emission sources determined from in-situ chemical measurements, Atmos. Chem. Phys., 13, 9337–9350, doi:10.5194/acp-13-9337-2013, 2013.

Chakrabarty, R. K., Moosmüller, H., Chen, L.-W. A., Lewis, K., Arnott, W. P., Mazzoleni, C., Dubey, M. K., Wold, C. E., Hao, W. M., and Kreidenweis, S. M.: Brown carbon in tar balls from smoldering biomass combustion, Atmos. Chem. Phys., 10, 6363–6370, doi:10.5194/acp-10-6363-2010, 2010.

Chen, Y. and Bond, T. C.: Light absorption by organic carbon from wood combustion, Atmos. Chem. Phys., 10, 1773–1787, doi:10.5194/acp-10-1773-2010, 2010.

Cheng, Y., He, K. B., Duan, F. K., Du, Z. Y., Zheng, M., and Ma, Y. L.: Characterization of carbonaceous aerosol by the stepwise-extraction thermal-optical-transmittance (SE-TOT) method, Atmos. Environ., 59, 551–558, 2012.

Cheng, Y., He, K.-B., Zheng, M., Duan, F.-K., Du, Z.-Y., Ma, Y.-L., Tan, J.-H., Yang, F.-M., Liu, J.-M., Zhang, X.-L., Weber, R. J., Bergin, M. H., and Russell, A. G.: Mass absorption efficiency of elemental carbon and water-soluble organic carbon in Beijing, China, Atmos. Chem. Phys., 11, 11497–11510, doi:10.5194/acp-11-11497-2011, 2011.

Cheng, Y., Engling, G., He, K.-B., Duan, F.-K., Ma, Y.-L., Du, Z.-Y., Liu, J.-M., Zheng, M., and Weber, R. J.: Biomass burning contribution to Beijing aerosol, Atmos. Chem. Phys., 13, 7765–7781, doi:10.5194/acp-13-7765-2013, 2013.

Chung, C. E., Kim, S.-W., Lee, M., Yoon, S.-C., and Lee, S.: Carbonaceous aerosol AAE inferred from in-situ aerosol measurements at the Gosan ABC super site, and the implications for brown carbon aerosol, Atmos. Chem. Phys., 12, 6173–6184, doi:10.5194/acp-12-6173-2012, 2012a.

Chung, C. E., Ramanathan, V., and Decremer, D.: Observationally constrained estimates of carbonaceous aerosol radiative forcing, P. Natl. Acad. Sci. USA, 109, 11624–11629, 2012b.

Clarke, A., McNaughton, C., Kapustin, V., Shinozuka, Y., Howell, S., Dibb, J., Zhou, J., Anderson, B., Brekhovskikh, V., Turner, H., and Pinkerton, M.: Biomass Burning and Pollution Aerosol over North America: Organic Components and Their Influence on Spectral Optical Properties and Humidification Response, J. Geophys. Res., 112, D12S18, doi:10.1029/2006jd007777, 2007.

DeCarlo, P. F., Kimmel, J. R., Trimborn, A., Northway, M. J., Jayne, J. T., Aiken, A. C., Gonin, M., Fuhrer, K., Horvath, T., Docherty, K. S., Worsnop, D. R., and Jimenez, J. L.: Field-Deployable,





ACPD
15, 28453–28482, 2015



High-Resolution Time-of-Flight Aerosol Mass Spectrometer, Anal. Chem., 78, 8281–8289, 2006.
Drewnick, F., Hings, S. S., DeCarlo, P., Jayne, J. T., Gonin, M., Fuhrer, K., Weimer, S., Jimenez, J. L., Demerjian, K. L., Borrmann, S., and Worsnop, D. R.: A new time-of-flight aerosol mass spectrometer (TOF-AMS)–Instrument description and first field deployment, Aerosol. Sci. Tech., 39, 637–658, 2005.
Du, Z., He, K., Cheng, Y., Duan, F., Ma, Y., Liu, J., and Weber, R.: A yearlong study of water-soluble organic carbon in Beijing I: Sources and its primary vs secondary nature, Atmos. Environ., 92, 514–521, 2014a.
Du, Z., He, K., Cheng, Y., Duan, F., Ma, Y., Liu, J., and Weber, R.: A yearlong study of water-soluble organic carbon in Beijing II: Light absorption properties, Atmos. Environ., 89, 235–241, 2014b.
Einfeld, W., Ward, D. E., and Hardy, C.: Effects of fire behavior on prescribed fire smoke characteristics: A case study, in: Global biomass burning: Atmospheric, climatic, and biospheric implications, MIT Press, Cambridge, MA, USA, 412–419, 1991.
Esposito, F., Calvello, M. R., Gueguen, E., and Pavese, G.: A new algorithm for brown and black carbon identification and organic carbon detection in fine atmospheric aerosols by a multi-wavelength Aethalometer, Atmos. Meas. Tech. Discuss., 5, 1003–1027, doi:10.5194/amtd-5-1003-2012, 2012.
Favez, O., Alfaro, S. C., Sciare, J., Cachier, H., Abdelwahab, M. M.: Ambient measurements of light-absorption by agricultural waste burning organic aerosols, J. Aerosol. Sci ., 40, 613–620, 2009.
Feng, Y., Ramanathan, V., and Kotamarthi, V. R.: Brown carbon: a significant atmospheric absorber of solar radiation?, Atmos. Chem. Phys., 13, 8607–8621, doi:10.5194/acp-13-8607-2013, 2013.
Fialho, P., Hansen, A. D. A., and Honrath, R. E.: Absorption coefficients by aerosols in remote areas: a new approach to decouple dust and black carbon absorption coefficients using seven wavelength Aethalometer data, J. Aerosol Sci., 36, 267–282, doi:10.1016/j.jaerosci.2004.09.004, 2005.
Gadhavi, H., Jayaraman, A.: Absorbing aerosols: contribution of biomass burning and implications for radiative forcing, Ann. Geophys., 28, 103–111, doi:10.5194/angeo-28-103-2010, 2010.





ACPD
15, 28453–28482, 2015



Gong, Z. H., Lan, Z. J., Xue, L., Zeng, L. W., He, L. Y., and Huang, X. F.: Characterization of submicron aerosols in the urban outflow of the central Pearl River Delta region of China, Environ. Sci. Eng., 6, 725–733, 2012.

Gyawali, M., Arnott, W. P., Lewis, K., and Moosmüller, H.: In situ aerosol optics in Reno, NV, USA during and after the summer 2008 California wildfires and the influence of absorbing and non-absorbing organic coatings on spectral light absorption, Atmos. Chem. Phys., 9, 8007–8015, doi:10.5194/acp-9-8007-2009, 2009.

Hansen, J., Sato, M., and Ruedy, R.: Radiative forcing and climate response, J. Geophys. Res., 102, 6831–6864, 1997.

Haywood, J. M., Roberts, D. L., Slingo, A., Edwards, J. M., and Shine, K. P.: General circulation model calculations of the direct radiative forcing by anthropogenic sulfate and fossil-fuel soot aerosol, J. Climate, 10, 1562–1577, 1997.

He, L.-Y., Lin, Y., Huang, X.-F., Guo, S., Xue, L., Su, Q., Hu, M., Luan, S.-J., and Zhang, Y.-H.: Characterization of high-resolution aerosol mass spectra of primary organic aerosol emissions from Chinese cooking and biomass burning, Atmos. Chem. Phys., 10, 11535–11543, doi:10.5194/acp-10-11535-2010, 2010.

He, L. Y., Huang, X. F., Xue, L., Hu, M., Lin, Y., Zheng, J., Zhang, R. Y., and Zhang, Y. H.: Submicron aerosol analysis and organic source apportionment in an urban atmosphere in Pearl River Delta of China using high-resolution aerosol mass spectrometry, J. Geophys. Res., 116, D12304, doi:10.1029/2010JD014566, 2011.

Herich, H., Hueglin, C., and Buchmann, B.: A 2.5 year's source apportionment study of black carbon from wood burning and fossil fuel combustion at urban and rural sites in Switzerland, Atmos. Meas. Tech., 4, 1409–1420, doi:10.5194/amt-4-1409-2011, 2011.

Huang, X.-F., He, L.-Y., Hu, M., Canagaratna, M. R., Kroll, J. H., Ng, N. L., Zhang, Y.-H., Lin, Y., Xue, L., Sun, T.-L., Liu, X.-G., Shao, M., Jayne, J. T., and Worsnop, D. R.: Characterization of submicron aerosols at a rural site in Pearl River Delta of China using an Aerodyne High-Resolution Aerosol Mass Spectrometer, Atmos. Chem. Phys., 11, 1865–1877, doi:10.5194/acp-11-1865-2011, 2011.

Huang, X. F., Sun, T. L., Zeng, L. W., Yu, G. H., and Luan, S. J.: Black carbon aerosol characterization in a coastal city in South China using a single particle soot photometer, Atmos. Environ., 51, 21–28, 2012.





ACPD
15, 28453–28482, 2015



Huang, X. F., Yun, H., Gong, Z. H., Li, X., He, L. Y., Zhang, Y. H., and Hu, M.: Source apportionment and secondary organic aerosol estimation of PM2.5 in an urban atmosphere in China, Science China: Earth Sciences, 57, 1352–1362, 2014.

Jacobson, M. Z.: Isolating nitrated and aromatic aerosols and nitrated aromatic gases as sources of ultraviolet light absorption, J. Geophys. Res., 104, 3527–3542, 1999.

Jacobson, M. Z.: Strong radiative heating due to the mixing state of black carbon in atmospheric aerosols, Nature, 409, 695–697, 2001.

Jayne, J. T., Leard, D. C., Zhang, X. F., Davidovits, P., Smith, K. A., Kolb, C. E., and Worsnop, D. R.: Development of an aerosol mass spectrometer for size and composition analysis of submicron particles, Aerosol. Sci. Tech., 33, 49–70, 2000.

Jethva, H. and Torres, O.: Satellite-based evidence of wavelength-dependent aerosol absorption in biomass burning smoke inferred from Ozone Monitoring Instrument, Atmos. Chem. Phys., 11, 10541–10551, doi:10.5194/acp-11-10541-2011, 2011.

Jimenez, J. L., Jayne, J. T., Shi, Q., Kolb, C. E., Worsnop, D. R., Yourshaw, I., Seinfeld, J. H., Flagan, R. C., Zhang, X. F., Smith, K. A., Morris, J. W., and Davidovits, P.: Ambient aerosol sampling using the Aerodyne Aerosol Mass Spectrometer, J. Geophys. Res., 108, 8425, doi:10.1029/2001JD001213, 2003.

Kirchstetter, T. W., Novakov, T., and Hobbs, P. V.: Evidence that the spectral dependence of light absorption by aerosols is affected by organic carbon, J. Geophys. Res., 109, D21, doi:10.1029/2004JD004999, 2004.

Kirillova, E. N., Andersson, A., Han, J., Lee, M., and Gustafsson, Ö.: Sources and light absorption of water-soluble organic carbon aerosols in the outflow from northern China, Atmos. Chem. Phys., 14, 1413–1422, doi:10.5194/acp-14-1413-2014, 2014.

Koch, D. and Hansen, J.: Distant origins of Arctic black carbon: a Goddard Institute for Space Studies ModelE experiment, J. Geophys. Res., 110, D04204, doi:10.1029/2004jd005296, 2005.

Lack, D. A. and Langridge, J. M.: On the attribution of black and brown carbon light absorption using the Ångström exponent, Atmos. Chem. Phys., 13, 10535–10543, doi:10.5194/acp-13-10535-2013, 2013.

Lack, D. A., Cappa, C. D., Cross, E. S., Massoli, P., Ahern, A. T., Davidovits, P., Onasch, T. B. : Absorption Enhancement of Coated Absorbing Aerosols: Validation of the Photo-Acoustic Technique for Measuring the Enhancement, Aerosol Sci. Tech., 43, 1006–1012, 2009.





ACPD
15, 28453–28482, 2015



Lack, D. A., Langridge, J., Richardson, M., Cappa, C. D., Law, D., and Murphy, D. M.: Aircraft instrumentation for comprehensive characterization of aerosol optical properties, Part 2: Black and brown carbon absorption and absorption enhancement measured with photo acoustic spectroscopy, Aerosol Sci. Tech., 46, 555–568, 2012a.

Lack, D. A., Langridge, J. M., Bahreini, R., Cappa, C. D., Middlebrook, A. M., and Schwarz, J. P.: Brown carbon and internal mixing in biomass burning particles, P. Natl. Acad. Sci. USA, 109, 14802–14807, doi:10.1073/pnas.1206575109, 2012b.

Lack, D. A., Moosmüller, H., McMeeking, G. R., Chakrabarty, R. K., and Baumgardner, D.: Characterizing elemental, equivalent black, and refractory black carbon aerosol particles: a review of techniques, their limitations and uncertainties, Anal. Bioanal. Chem., 406, 99–122, doi:10.1007/s00216-013-7402-3, 2014.

Lan, Z. J., Chen, D. L., Li, X., Huang, X. F., He, L. Y., Deng, Y. G., Feng, N., and Hu, M.: Modal characteristics of carbonaceous aerosol size distribution in an urban atmosphere of South China, Atmos. Res., 100, 51–60, 2011.

Lan, Z. J., Huang, X. F., Yu, K. Y., Sun, T. L., Zeng, L. W., and Hu, M.: Light absorption of black carbon aerosol and its enhancement by mixing state in an urban atmosphere in South China, Atmos. Environ., 69, 118–123, 2013.

Levin, E. J. T., McMeeking, G. R., Carrico, C. M., Mack, L. E., Kreidenweis, S. M. Word, C. E., Moosmuller, H., Arnott, W. P., Hao, W. M., Cottett Jr, J. L., and Malm, W. C.: Biomass burning smoke aerosol properties measured during Fire Laboratory at Missoula Experiments (FLAME), J. Geophys. Res.-Atmos., 115, D182010, doi:10.1029/2009JD013601, 2010.

Lewis, K., Arnott, W. P., Moosmuller, H., and Wold, C. E.: Strong spectral variation of biomass smoke light absorption and single scattering albedo observed with a novel dual-wavelength photoacoustic instrument, J. Geophys. Res., 113, D16, doi:10.1029/2007JD009699, 2008.

McNaughton, C. S., Clarke, A. D., Freitag, S., Kapustin, V. N., Kondo, Y., Moteki, N., Sahu, L., Takegawa, N., Schwarz, J. P., Spackman, J. R., Watts, L., Diskin, G., Podolske, J., Holloway, J. S., Wisthaler, A., Mikoviny, T., de Gouw, J., Warneke, C., Jimenez, J., Cubison, M., Howell, S. G., Middlebrook, A., Bahreini, R., Anderson, B. E., Winstead, E., Thornhill, K. L., Lack, D., Cozic, J., and Brock, C. A.: Absorbing aerosol in the troposphere of the Western Arctic during the 2008 ARCTAS/ARCPAC airborne field campaigns, Atmos. Chem. Phys., 11, 7561–7582, doi:10.5194/acp-11-7561-2011, 2011.





ACPD
15, 28453–28482, 2015



Miyazaki, Y., Kondo, Y., Han, S., Koike, M., Kodama, D., Komazaki, Y., and Matsueda, H.: Chemical characteristics of water-soluble organic carbon in the Asian outflow, J. Geophys. Res., 112, D22, doi:10.1029/2007JD009116, 2007.

Moosmuller, H., Arnott, W. P., Rogers, C. F., Chow, J. C., Frazier, C. A., Sherman, L. E., and Dietrich, D. L.: Photoacoustic and filter measurements related to aerosol light absorption during the Northern Front Range Air Quality Study (Colorado 1996/1997), J. Geophys. Res., 103, 28149–28157, 1998.

Nakayama, T., Ikeda, Y., Sawada, Y., Setoguchi, Y., Ogawa, S., Kawana, K., Mochida, M., Ikemori, F., Matsumoto, K., and Matsumi, Y.: Properties of light-absorbing aerosols in the Nagoya urban area, Japan, in August 2011 and January 2012: Contributions of brown carbon and lensing effect, J. Geophys. Res. Atmos., 119, 12721–12739, doi:10.1002/2014JD021744, 2014.

Ng, N. L., Herndon, S. C., Trimborn, A., Canagaratna, M. R., Croteau, P. L., Onasch, T. B., Sueper, D., Worsnop, D. R., Zhang, Q., Sun, Y. L., and Jayne, J. T.: An Aerosol Chemical Speciation Monitor (ACSM) for routine monitoring of the composition concentrations of ambient aerosol, Aerosol Sci. Tech., 45, 770–784, 2011.

Patterson, E. M. and McMahon, C. K.: Absorption characteristics of forest fire particulate matter, Atmos. Environ., 18, 2541–2551, 1984.

Poschl, U.: Atmospheric Aerosols: Composition, Transformation, Climate, and Health Effects, Atoms. Chem., 44, 7520–7540, 2005.

Ramanathan, V. and Carmichael, G.: Global and regional climate changes due to black carbon, Nat. Geosci., 1, 221–227, 2008.

Sandradewi, J., Prév^t, A. S. H., Alfarra, M. R., Szidat, S., Wehrli, M. N., Ruff, M., Weimer, S., Lanz, V. A., Weingartner, E., Perron, N., Caseiro, A., Kasper-Giebl, A., Puxbaum, H., Wacker, L., and Baltensperger, U.: Comparison of several wood smoke markers and source apportionment methods for wood burning particulate mass, Atmos. Chem. Phys. Discuss., 8, 8091–8118, doi:10.5194/acpd-8-8091-2008, 2008a.

Sandradewi, J., Prevot, A. S. H., Szidat, S., Perron, N., Alfarra, M. R., Lanz, V. A., Weingartner, E., and Baltensperger, U.: Using Aerosol Light Absorption Measurements for the Quantitative Determination of Wood Burning and Traffic Emission Contributions to Particulate Matter, Envir. Sci. Tech., 42, 3316–3323, doi:10.1021/es702253m, 2008b.





ACPD
15, 28453–28482, 2015



Sandradewi, J., Prevot, A. S. H., Weingartner, E., Schmidhauser, R., Gysel, M., and Baltensperger, U.: A study of wood burning and traffic aerosols in an Alpine valley using a multi-wavelength Aethalometer, Atmos. Environ., 42, 101–111, 2008c.

Scarnato, B. V., Vahidinia, S., Richard, D. T., and Kirchstetter, T. W.: Effects of internal mixing and aggregate morphology on optical properties of black carbon using a discrete dipole approximation model, Atmos. Chem. Phys., 13, 5089–5101, doi:10.5194/acp-13-5089-2013, 2013.

Schmid, O., Artaxo, P., Arnott, W. P., Chand, D., Gatti, L. V., Frank, G. P., Hoffer, A., Schnaiter, M., and Andreae, M. O.: Spectral light absorption by ambient aerosols influenced by biomass burning in the Amazon Basin. I: Comparison and field calibration of absorption measurement techniques, Atmos. Chem. Phys., 6, 3443–3462, doi:10.5194/acp-6-3443-2006, 2006.

Streets, D. G., Gupta, S., Waldhoff, S. T., Wang, M. Q., Bond, T. C., and Bo, Y. Y.: Black carbon emissions in China, Atmos. Environ., 35, 4281–4296, 2001.

Sun, H., Biedermann, L., and Bond, T. C.: Color of brown carbon: A model for ultraviolet and visible light absorption by organic carbon aerosol, Geophys. Res. Lett., 34, L17813, doi:10.1029/2007GL029797, 2007.

Wang, L., Li, Z. Q., Tian, Q. J., Ma, Y., Zhang, F. X., Zhang, Y., Li, D. H., Li, K. T., and Li, L.: Estimate of aerosol absorbing components of black carbon, brown carbon, and dust from ground-based remote sensing data of sun-sky radiometers, J. Geophys. Res., 118, 6534–6543, doi:10.1002/jgrd.50356, 2013.

Wang, X., Doherty, S. J., and Huang, J.: Black carbon and other light-absorbing impurities in snow across Northern China, J. Geophys. Res., 118, 1471–1492, doi:10.1029/2012jd018291, 2013.

Wang, X., Heald, C. L., Ridley, D. A., Schwarz, J. P., Spackman, J. R., Perring, A. E., Coe, H., Liu, D., and Clarke, A. D.: Exploiting simultaneous observational constraints on mass and absorption to estimate the global d irect radiative forcing of black carbon and brown carbon, Atmos. Chem. Phys., 14, 10989–11010, doi:10.5194/acp-14-10989-2014, 2014.

Washenfelder, R. A., Attword, A. R., Brock, C. A., Guo, H., Xu, L., Weber, R. J., Ng, N. L., Allen, H. M., Ayres, B. R., Baumann, K., Cohen, R. C., Draper, D. C., Duffey, K. C., Edgerton, E., Fry, J. L., Hu, W. W., Jimenez, J. L., Palm, B. B., Romer, P., Stone, E. A., Wooldridge, P. J., and Brown, S. S.: Biomass burning dominates brown carbon absorption in the rural southeastern United States, Geophys. Res. Lett., 42, 653–664, doi:10.1002/2014GL062444, 2015.





ACPD
15, 28453–28482, 2015



Yang, M., Howell, S. G., Zhuang, J., and Huebert, B. J.: Attribution of aerosol light absorption to black carbon, brown carbon, and dust in China – interpretations of atmospheric measurements during EAST-AIRE, Atmos. Chem. Phys., 9, 2035–2050, doi:10.5194/acp-9-2035-2009, 2009.

Yuan, Z. B., Lau, A. K. H., Zhang, Y. H., Yu, J. Z., Louie, P. K. K., and Fung, J. C. H.: Identification and spatiotemporal variations of dominant PM10 sources over Hong Kong, Atmos. Environ., 40, 1803–1815, 2006.

Zhang, Y. H., Hu, M., Liu, S. C., and Wiedensohler, A.: The special issue on PRIDE-PRD2004 campaign, Atmos. Environ., 42, 6155–6156, 2008.





ACPD
15, 28453–28482, 2015



**Table 1.** The calibration results of PASS-3 in the campaigns.

| Campaign | Flow rate (lpm) | Error of laser power_405 nm | Error of laser power_532 nm | Error of laser power_781 nm | Slope ($R^2$) |
|---|---|---|---|---|---|
| $Urban_{\_winter}$ | 0.97 | 0.6 (%) | 2.3 (%) | 2.5 (%) | 1.02 (0.995) |
| $Urban_{\_fall}$ | 0.98 | 4.0 (%) | 1.1 (%) | 0.9 (%) | 1.03 (0.996) |
| $Rural_{\_fall}$ | 0.98 | 2.5 (%) | 5.0 (%) | 3.6 (%) | 1.04 (0.993) |
| Tunnel | 0.98 | 2.5 (%) | 5.0 (%) | 3.6 (%) | 1.04 (0.993) |





ACPD
15, 28453–28482, 2015



**Table 2.** The derived $AAE_{BC}$ values and uncertainties in the campaigns.

| Campaign | $AAE_{405\_781}$ | $AAE_{532\_781}$ |
|---|---|---|
| $Urban_{\_winter}$ | $0.86 \pm 0.06$ | $0.70 \pm 0.05$ |
| $Urban_{\_fall}$ | $0.82 \pm 0.06$ | $0.71 \pm 0.06$ |
| $Rural_{\_fall}$ | $1.02 \pm 0.10$ | $0.86 \pm 0.13$ |





ACPD
15, 28453–28482, 2015



**Table 3.** The derived $AAE_{BC}$ values and uncertainties in the tunnel experiments.

| Tunnel | $AAE_{405\_781}$ | $AAE_{532\_781}$ |
|---|---|---|
| TL-1 | $0.85 \pm 0.06$ | $0.72 \pm 0.10$ |
| TL-2 | $0.80 \pm 0.11$ | $0.68 \pm 0.19$ |
| JW | $0.89 \pm 0.06$ | $0.63 \pm 0.12$ |





ACPD
15, 28453–28482, 2015



**Table 4.** The AAE values observed in the biomass burning simulation experiments.

| Biomass type | Burning modes | $AAE_{405\_781}$ | $AAE_{532\_781}$ | $AAE_{405\_532}$ |
|---|---|---|---|---|
| Ficus microcarpa leaf | | 4.46 ± 1.20 | 3.46 ± 0.96 | 5.85 ± 1.69 |
| Lychee leaf | | 3.48 ± 1.20 | 2.52 ± 1.07 | 4.90 ± 1.61 |
| Corn stalk | | 2.97 ± 1.16 | 2.39 ± 1.06 | 3.83 ± 1.49 |
| Peanut stalk | Stove burning | 1.99 ± 0.50 | 2.08 ± 0.86 | 2.13 ± 1.01 |
| Litchi wood | | 2.61 ± 1.00 | 1.95 ± 0.85 | 3.55 ± 1.50 |
| Eucalyptus wood | | 1.71 ± 0.50 | 1.30 ± 0.53 | 2.34 ± 0.85 |
| Short straw | | 1.76 ± 0.25 | 1.39 ± 0.47 | 2.32 ± 0.65 |
| Short straw | Open burning | 6.20 ± 1.33 | 4.96 ± 1.15 | 8.27 ± 1.34 |





ACPD
15, 28453–28482, 2015



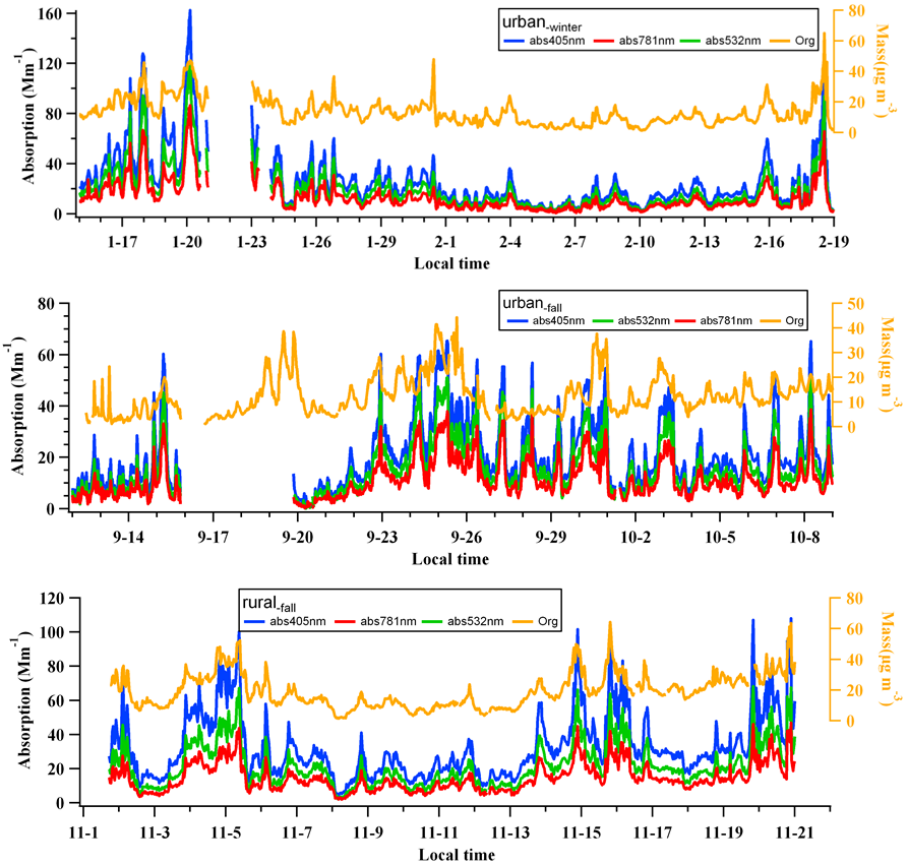


**Figure 1.** The time series of aerosol light absorption and mass concentration of organic aerosol in different campaigns.





ACPD
15, 28453–28482, 2015



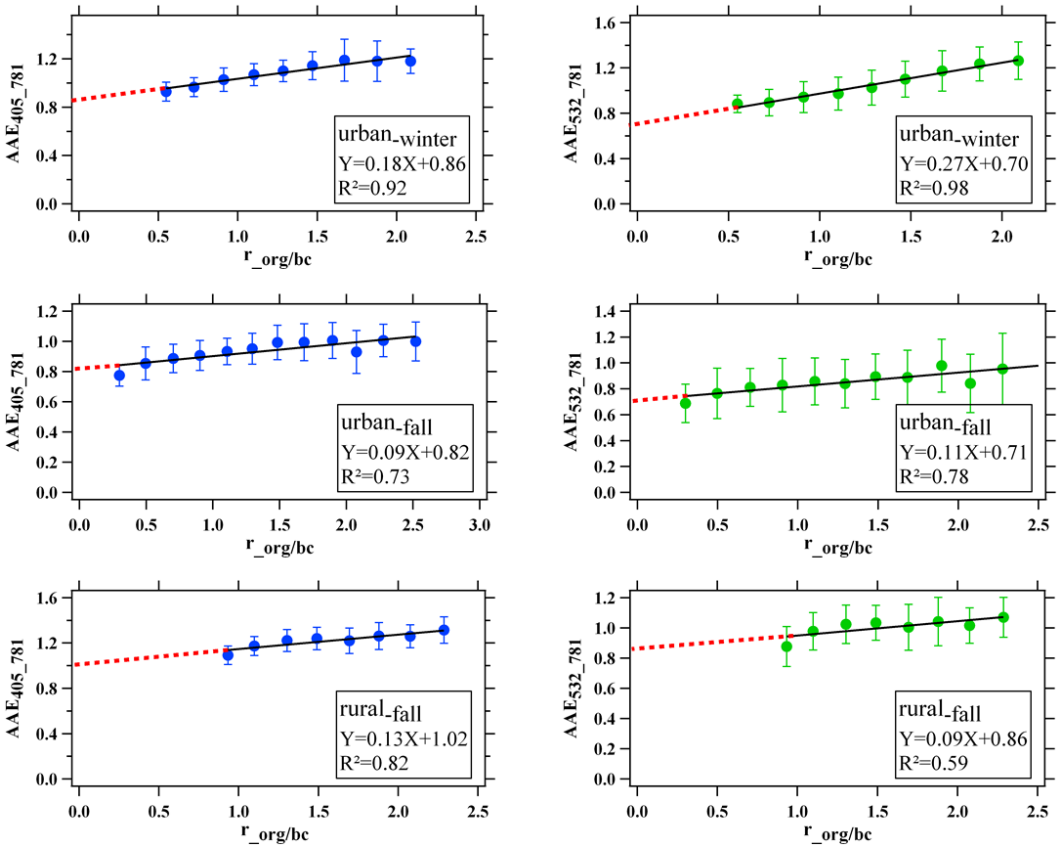


**Figure 2.** The linear relationship between AAE and $r_{org/bc}$ in different campaigns.





ACPD
15, 28453–28482, 2015



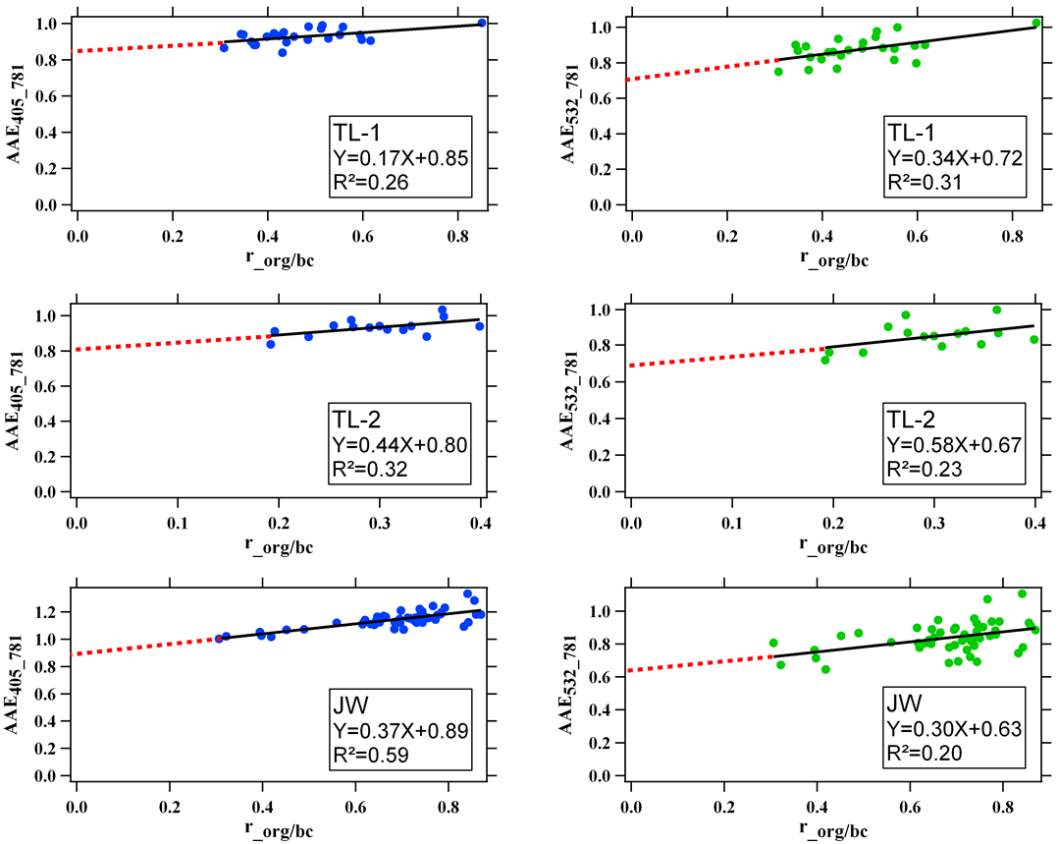


**Figure 3.** The linear relationship between AAE and $r_{org/bc}$ in the tunnel experiments.





ACPD
15, 28453–28482, 2015